

**Backward Raman amplification in a partially ionized gas**A. A. Balakin,<sup>1</sup> G. M. Fraiman,<sup>1</sup> N. J. Fisch,<sup>2</sup> and S. Suckewer<sup>3</sup><sup>1</sup>*Institute of Applied Physics, RAS, Nizhnii Novgorod, Russia 603950*<sup>2</sup>*Department of Astrophysical Science, Princeton University, Princeton, New Jersey 08543, USA*<sup>3</sup>*Department of Mechanical and Aerospace Engineering, Princeton University, Princeton, New Jersey 08543, USA*

(Received 30 March 2005; published 2 September 2005)

Compressing laser pulses to extremely high intensities through backward Raman amplification might be accomplished in a plasma medium. While the theory is relatively straightforward for homogeneous fully ionized plasma, a number of important effects enter when the plasma is not fully ionized. In particular, when a mixture of gases is employed to accomplish the coupling, there can be several thresholds for incremental ionization. The refraction of both the pump and the seed is then strongly affected by the plasma ionization. Moreover, in the case of Raman backscattering in partially ionized plasma, the degree of plasma ionization is particularly sensitive to the counterpropagating geometry. This idea is examined in light of data for a recent experiment on a Raman amplifier.

DOI: [10.1103/PhysRevE.72.036401](https://doi.org/10.1103/PhysRevE.72.036401)

PACS number(s): 52.38.-r, 42.65.Dr, 52.65.-y, 52.70.-m

**I. INTRODUCTION**

Compressing laser pulses to extremely high intensities, overcoming the material limits of conventional compression techniques, may be possible through plasma-mediated mechanisms. The most advanced mechanism involves resonant Raman backscattering (RBS) in the pump-depletion regime [1,2]. Other coupling techniques involving plasma include Compton scattering [3] and Raman backscattering at an ionization front [4]. The resonant RBS regime is attractive because it is one of the simplest resonant interactions in plasma. This interaction dominates deleterious competing instabilities [1]. The seed can maintain focusability [5], superluminous precursor solutions [6] can be avoided, and there are a variety of realizable highly compressed ultrashort pulse solutions [7]. Techniques for delivering power conveniently through multiple pumps also appear to be feasible [8]. The extent to which the amplification process tolerates an inhomogeneous plasma was recently formulated as well [9].

The resonant Raman backscattering technique has recently enjoyed experimental success, wherein the pump-depletion regime was accessed [10,11]. The experimental success was achieved using a gas jet of propane, subsequently ionized, creating a target plasma. The counterpropagating laser beams then were coupled in the ionized target plasma.

However, though the nonlinear pump-depletion regime was accessed by these experiments, the regime itself was not fully explored in the regime where the pump depletion was very significant, that is, where there was high efficiency in the conversion of pump energy to a backscattered compressed pulse. The reason for this likely resides in the imperfect target plasma, which was not the homogeneous fully ionized plasma that would be most desired. Using the propane gas jet, as opposed to pure hydrogen, eased conditions on the gas jet nozzle, since a lower gas pressure could produce a higher density target. However, the use of propane opens up the question of coupling in a partially ionized gas.

Any additional ionization during the RBS amplification process changes several aspects of the problem. Additional

ionization might be put to use by suppressing noise [12]. If all the plasma is created by the seed pulse, then there exists the possibility to create the coupling at an ionization front [2,13,14].

However, except for the highly controlled cases above, in general, additional ionization is deleterious. First, depending on the nature of the ionization, there can be plasma density perturbations even if the plasma or gas was initially homogeneous. These plasma density perturbations then can refract both the pump and the seed. This leads to the spreading out of the pump energy from one side and the effective decreasing of the seed amplification from the other side. Second, the additional ionization breaks the resonance condition between pump and seed. The seed amplitude will then saturate at the ionization threshold.

One peculiarity of the field ionization is that the rate of ionization depends exponentially on total field amplitude. Thus, the time averaged ionization values will depend on the maximum amplitudes resulting from the superposition of both the pump and seed fields. The effective intensity of the superposition is the square of the sum of the square roots from pump and seed intensities. It means that even a small value of the seed intensity will change the total intensity by a significant amount. For example, a seed intensity at 10% of the pump intensity in a counterpropagating geometry ionizes as effectively as a pump with an intensity 1.7 times greater, but in the absence of the counterpropagating seed. Due to this strong dependence on the field intensity, one can find that, in complex gases (like propane  $C_3H_8$ ), additional electrons appear when the pump intensity is less than the ionization threshold, thus providing additional ionization of higher  $Z$  atoms which may increase seed and pump refraction.

This paper is organized as follows. In Sec. II we describe the equations employed in our computer simulation. In Sec. III we consider the RBS amplification in the case of partially ionized gases in a one-dimensional (1D) simulation. In Sec. IV we show how any inhomogeneity of the gas, or plasma density, or electromagnetic pulses affects the seed profile. We suggest also the method of the seed intensity diagnostic using additional ionization. In Sec. V we present 2D simula-

tions of a long-duration pump in propane, which is being additionally ionized by the pump pulse. The formation of a channel-like structure is demonstrated. In Sec. VI we suggest how these conclusions may bear on recent experiments. In Sec. VII we conclude by suggesting a number of practical recommendations for backward Raman amplification.

## II. BASIC EQUATIONS AND CODE OUTLINE

The numerical scheme involves solving the two-dimensional equations describing the three-wave interaction process [2]

$$\partial_t a + \partial_z a - i\nabla_{\perp}^2 a + i\kappa \delta n a = b f, \quad (1)$$

$$\partial_t b - \partial_z b - i\nabla_{\perp}^2 b + i\kappa \delta n b = -a f^*, \quad (2)$$

$$\partial_t f + i\kappa \delta n f = -a b^*, \quad (3)$$

where  $a$  and  $b$  are the amplitudes of the vector potentials of the pump wave and the amplified pulse, respectively, measured in units of  $m_e c \omega_0 / e$ ,  $f$  is the amplitude of the plasma wave electric potential measured in units of  $(m_e c \omega_0 / 2e) \sqrt{\omega_p / 2\omega_0}$ , and the pump frequency  $\omega_0$  is much larger than the resonant plasma frequency<sup>1</sup>  $\omega_p = \sqrt{4\pi n_{\Delta} e^2 / m_e}$  and can be considered in all these coefficients equal to the amplified pulse frequency,  $e$  and  $m$  are the electron charge and mass, respectively; the time  $t$  is measured in units of  $t_0 = \sqrt{2 / \omega_0 \omega_p}$ , the longitudinal coordinate  $z$  is measured in units of  $ct_0$ , the detuning  $\delta\omega$  is measured in units of  $t_0^{-1}$ . The coefficients  $\kappa$  and  $\varkappa$  are

$$\kappa = \sqrt{\frac{2\omega_p}{\omega}}, \quad \varkappa = 2 \left( \frac{\omega_p}{2\omega} \right)^{3/2}. \quad (4)$$

The plasma density

$$\delta n = \sum q n_q - n_{\Delta} \quad (5)$$

is determined from the system of equations

$$\partial n_0 / \partial t = -w_1 n_1, \quad (6)$$

$$\partial n_q / \partial t = w_q n_{q-1} - w_{q+1} n_q, \quad q > 0, \quad (7)$$

where  $n_{q=0}$  is the neutral density and  $n_{q>0}$  is the density of the  $q$ -times ionized atoms. The ionization rate  $w_q$  is determined by the relation [15]

$$w_q = C_q \left( \frac{a_q}{a} \right)^{2n_q - 3/2} \exp\left(-\frac{2a_q}{3a}\right), \quad (8)$$

where

$$N_q = \sqrt{U_H / U_q},$$

$$C_q = \sqrt{\frac{3}{\pi}} \frac{\omega_H U_q}{\omega U_H} (4e)^{2N_q} \frac{1}{2\pi n_q N_q^{N_q}},$$

<sup>1</sup>Note that this plasma frequency, based upon the plasma density  $n_{\Delta}$ , is not the local plasma frequency; rather it is the necessary plasma frequency for resonant interaction.

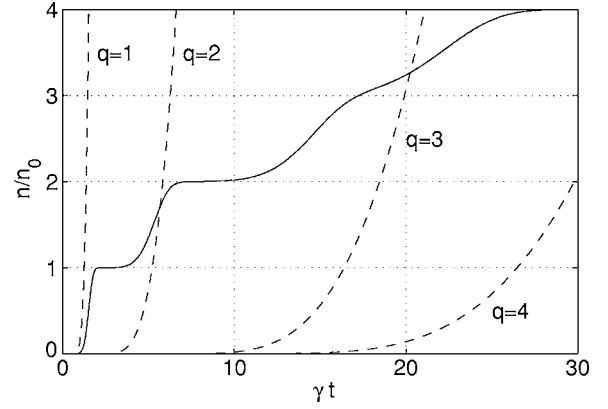


FIG. 1. The dependence of the carbon plasma density vs time for the case when the amplitude of the electric field grows linearly in time,  $a = a_0 \times \gamma t$ . Dashed lines show the ionization rates  $w_q$  for corresponding stages  $q = 1, \dots, 4$ .

$$a_q = 0.3 \times (U_q / U_H)^{3/2} / \omega a_0,$$

$U_q$  is the ionization potential for the  $q$ (th) ionization stage,  $U_H \approx 13.6$  eV is the ionization potential for hydrogen, and  $\omega_H \approx 4.1 \times 10^{16}$  Hz is the atomic frequency. We consider only the field ionization since the time of the impact ionization is small in comparison to the characteristic time of the RBS (several picoseconds).

An example of the plasma density evolution versus amplitude of the electric field is presented in Fig. 1 for carbon gas. It is seen that the dependence of the plasma density in time has the form of a “step” for the first two stages of ionization. However, the further change of the density from the third to the fourth stage of the ionization is smooth. The fourth stage of the ionization is clearly observed. This character of the density dependence is typical for many gases. It can be understood as follows. The relative difference of the ionization potential for the first three ionization stages is significant (for information, the ionization potentials of carbon are 11, 24, 48, 64, 380, and 470 eV). Each of these stages has at least twice higher ionization potential than the previous one. In contrast, the relative difference of the third and fourth ionization potentials is small. So, the third-stage ionized ions have the possibility to be ionized to the fourth stage even when not all the plasma is ionized to the third stage. Between the fourth and fifth ionization stages lies a sufficient gap so that ionization to the fifth stage is delayed. The gap arises because the fifth stage is formed by  $s$  electrons which are more difficult to ionize.

The dependence of the ionization rate versus instantaneous field amplitude is illustrated in Fig. 1. Since density is time dependent, we use a slowly varying electric field (linearly in time). Thus, the axis of Fig. 1 can be taken as time, or effectively as field amplitude. Significant growth of the ionization rate  $w_q$  takes place for low stages of ionization. As a result, the plasma ionizes at each corresponding stage of the ionization before the next stage ionization become possible. At the same time, the ionization rate of the fourth stage overlaps the third one. So the passage from the twofold ionized to the fourfold ionized plasma proceeds smoothly.

In the calculations presented below the pump wave amplitude is  $a_0=0.006$  and it has a Gaussian transverse profile with various widths; the pump wavelength is  $\lambda=0.8 \mu\text{m}$  (the frequency is  $\omega_0=2.36 \times 10^{15} \text{ sec}^{-1}$ ). For such parameters, the linear  $e$ -folding length, calculated according to the linear growth rate of the monochromatic pump backscattering instability  $\gamma=a_0\sqrt{\omega_0\omega_p}/2$ , is  $c/\gamma=130 \mu\text{m}$ . We used the length of the plasma 7 mm or  $55c/\gamma$ . The initial seed pulse had the same transverse Gaussian profile as the pump, but a twice smaller amplitude and a duration of 40 fs ( $12 \mu\text{m}$  length):

$$b_0 = \frac{a_0}{2} e^{-(t/40 \text{ fs})^2/2} F(r), \quad F(r) = e^{-(r/10 \text{ cm})^2/2}. \quad (9)$$

Numerical simulations were performed with the hydrodynamic code MRBS [8] which was created specifically for RBS amplification simulation.

One should note two important features of the field ionization. The first one is well known—we mean the threshold character of the effect, i.e., even small variation of the field amplitude might sufficiently increase the ionization probability. The second feature is that the ionization is caused by the instantaneous field amplitude. In particular, this means that if there are two waves with intensities  $I_1 \gg I_2$  then the effective intensity of the ionizing field  $I_{\text{eff}}$  is equal to

$$I_{\text{eff}} - I_1 \approx 2\sqrt{I_1 I_2} \gg I_2,$$

which together with the threshold character of the effect allows one to have noticeable ionization at small levels of  $I_2$  even if intensities  $I_1$  and  $I_1+I_2$  are lower than the ionization threshold.

### III. SATURATION DUE TO IONIZATION

The problem that ionization presents is density growth which leads to resonance detuning after the beginning of the ionization, or defocusing. Consider, for example, additional ionization of the plasma during RBS amplification, for example, in pure helium or carbon plasmas (see Fig. 2). Then after some amplification, the seed amplitude causes additional ionization, which disrupts the amplification of the central and tail seed parts. This disruption always occurs for gases containing ions of only one species because after ionization the plasma frequency becomes twice larger than optimal, breaking the resonance condition. It is easy to estimate the maximum intensity for the beginning of the additional ionization with ionizing potential  $U_q$  (in eV):

$$a_q \approx 0.006 \left( \frac{U_q}{U_H} \right)^{3/2}, \quad (10)$$

where the coefficient is determined from the numerical simulation.

Although a seed with shifted initial frequency which is not optimal for the initial plasma density may appear to be useful, it turns out not quite so. Unfortunately this initial detuning of the seed does not lead to a resonant interaction upon further ionization. The saturation occurs because of the smallness of the inverse increment in comparison with the plasma frequency. The seed frequency detuning cannot ex-

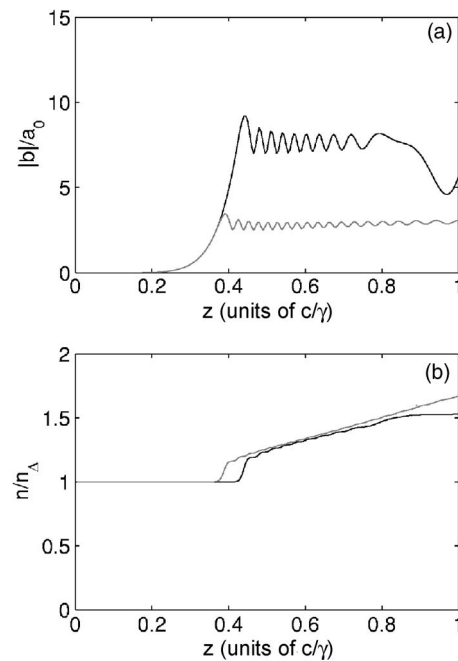


FIG. 2. This figure shows the appearance of the detuning due to increase of the plasma density. The seed and the pump propagate in initially once ionized helium (black) or carbon (gray).

ceed several inverse increments  $\delta\omega \leq \gamma$ , for the RBS scheme to be efficient. The ionization increases the plasma frequency by an amount on the order of the plasma frequency  $\omega_p \gg \gamma$ , so that gain is saturated.

One should note that at longer times the simulation using Eqs. (1) shows the appearance of a signal which is resonant with the increased density at the tail of the seed. As a result there is some further amplification of this frequency-shifted signal. Unfortunately Eqs. (1) are applicable only for small enough density perturbations (less than  $n_\Delta$ ). For large density perturbations, there may be other backscattered light that we are not considering accurately through our three-wave envelope approximation. Thus, our simulation can describe qualitatively but not exactly the evolution of the frequency-shifted signal or, for that matter, any ionization processes that will be due to the frequency-shifted signal.

The process works as follows. Due to ionization, the seed spectrum broadens. Very weak harmonics appear, resonant with newly produced plasma density, which can then be amplified. However, this ideal “transformation” has several limitations. The first one is due to the necessity of preventing the density growth during these weak harmonic amplifications, i.e., it needs time for full ionization of the plasma at some stage. The second one is related to turning on of the next stages of ionization (third, fourth, and so on). The problem is that even small amplification of shifted harmonics on a background of existing seed amplitude will exceed the ionization threshold and breaks amplification again.

To escape such detuning one can use fully ionized gas with large preionization stage before beginning of the RBS amplification process, or gases containing a sufficient portion of the hydrogen ions—any organic gases, for example. For the first two cases, there is no additional ionization during

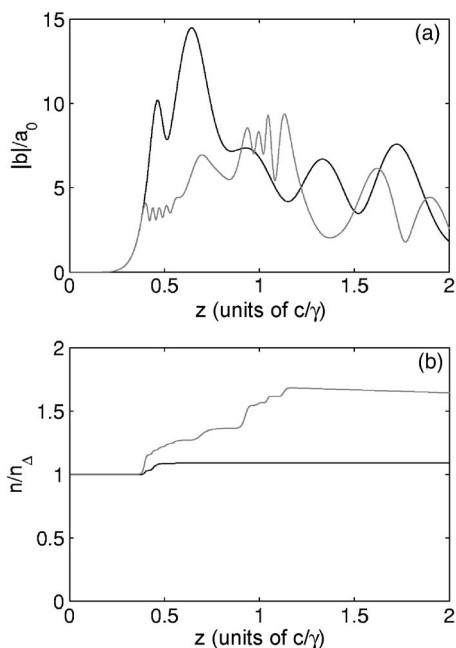


FIG. 3. This is RBS amplification simulation in hydrogen plasma with small admixture of carbon ions (near 3% of the ions, black) and in propane gas ( $C_3H_8$ ), gray). These cases differ in the ratio of the additionally produced plasma in comparison with the existing one. As a result the second stage of the ionization is reached at different rates and with different amplification.

RBS amplification so the detuning effect due to ionization is absent.

The third case is a bit more complex. For a gas  $A_xH_y$  with single ionized  $A$  ( $A$  means any type of atom) and hydrogen  $H$  we note a relative increase of the density of the order (due to the next stage of ionization of  $A$ ):

$$\frac{\delta n}{n_0} \approx \frac{x}{x+y}. \quad (11)$$

Suppose this ratio stays less than the detuning condition

$$\frac{\delta n}{n_\Delta} \leq \frac{2\gamma}{\omega_p} = a_0 \sqrt{\frac{2\omega}{\omega_p}}. \quad (12)$$

One can choose methane  $CH_4$  or another gas with a small quantity of carbon atoms in the molecule. Often propane gas ( $C_3H_8$ ) is used in experiment due to its easy accessibility and high density of the produced plasma.<sup>2</sup> However even in this case one should be aware of the additional ionization because of the possibility realization of the detuning condition.

For example, in Fig. 3 one can see RBS amplification simulation in hydrogen plasma with a small admixture of carbon ions (about 3%). The appearance of the double ionized carbon ions in this blend does not break down the reso-

<sup>2</sup>Each molecule of propane produces  $3+8=11$  ions. As a result, for similar pressure of the gases the plasma density becomes higher.

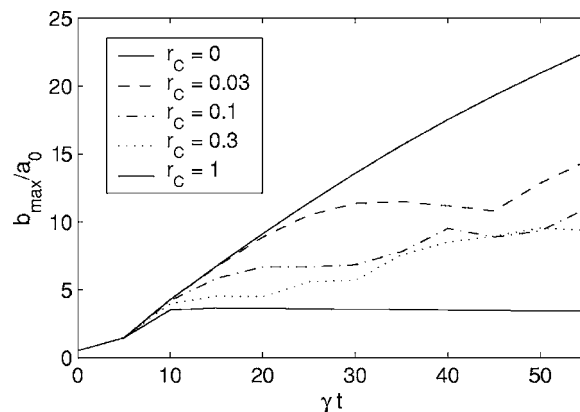


FIG. 4. The growth law for the seed amplitude vs time. It is seen that the presence of the additional ionization decreases the seed amplitude and causes the “steppedlike” form of the growth law.

nance condition (12).<sup>3</sup> As a result the amplification in the central part continues. But the appearance of the third- and fourth-time ionized carbon ions breaks down the resonance condition (12) and stops the amplification.

It is interesting that the appearance of the frequency-shifted signal at the tail of the seed can produce some extra amplification in the case of a two-component plasma (for example, in propane gas  $C_3H_8$ ). One can see that the additional density  $\delta n/n_0 = 3/11 \approx 0.27$  is larger than the detuning condition. But the appearance of the frequency-shifted part of the seed allows further amplification. When the seed amplitude reaches the level of the third ionization stage of the carbon the additional ionization again stops further amplification of the frequency-shifted part. But again there will be frequency-shifted signals now in resonance which can now undergo amplification. Thus the process of amplification of shifted radiation repeats at this higher ionization state. So the situation repeats.

Also note that the seed duration increases during RBS amplification. It happens because the frequency-shifted signal needs some distance (time) to be amplified up to a non-linear level. Therefore the compression of the amplified pulse become worse if there is additional ionization present.

Figure 3 demonstrates this fact in the case of propane gas ( $C_3H_8$ ). One can see structure as in the case of helium gas at the leading edge. But there also appears an intense part at the center of the seed. The growth of this part is stabilized by producing the third ionization of carbon ions. However a small concentration of ions in the fourth ionization stage can be seen at the tail of the seed. As a result the growth rate of the seed amplitude becomes nonlinear (as in the  $\pi$ -pulse solution) but of stepped form (Fig. 4). From Fig. 4 it is clear that the increase of the amount of carbon admixture leads to decreasing of the Raman amplification.

#### IV. SEED REFRACTION

Seed refraction often accompanies ionization for narrow beams, destroying the phase coherency of the pulse. The

<sup>3</sup>Here we do not discuss the focusing of the seed after the amplification [8,9].

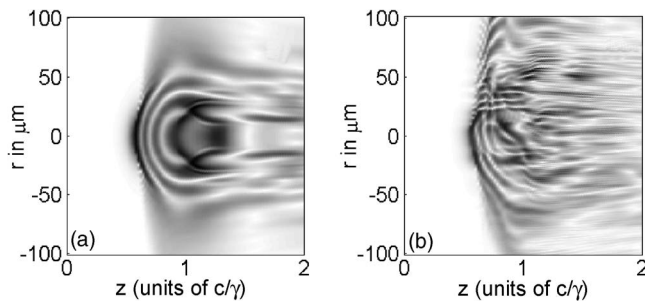


FIG. 5. Example of the seed refraction in the case of a smooth (left) and a nonsmooth pump (right). Seed and pump have transverse size  $60 \mu\text{m}$  full width at half maximum (FWHM). The “nonsmooth” pump is formed by three beams with slightly different frequencies  $\Delta\omega = \gamma$ .

density increase leads not only to breaking of the RBS resonance condition but also to transverse modulation of the phase and amplitude profile. Furthermore, the refraction will be accompanied by a spreading of the pulse power over a larger area, leading to a decrease in the seed intensity.

This spreading is even more dangerous since it may be caused by any inhomogeneity of the medium or the pump or seed. Even if the inhomogeneity by itself would not lead to reflection, the inhomogeneity in partially ionized plasma is more dangerous. The reason is that the field ionization occurs in steps.

For example, using a pump containing several beams keeps the seed focusability in the absence of ionization [8]. Note that even using a pump that is poor quality or with a jagged intensity profile will also keep the seed focusability. But the presence of the additional ionization will change the picture dramatically. In speckles (where the pump amplitude reaches maximum) the ionization happens much earlier. This leads to the plasma being produced in the presence of an intensive enough seed. This plasma will refract the seed itself. As a result the homogeneity can be achieved only on at the leading edge (see Fig. 5). Nevertheless in the absence of ionization the transverse profile of the seed is smooth. Note that this speculation is correct only for narrow speckles. The use of the sufficiently small angular pump spreading (or larger transverse size of the speckles) will suppress refraction and keep the seed focusable.

The similar effect takes place in the case of an inhomogeneous plasma. The probability of ionization is the same for all points of the seed leading edge. But the value of the plasma produced is different from point to point. As a consequence the plasma density fluctuates and seed refraction appears (see Fig. 6).

Thus the seed ionization leads to “modulative distortion” of the seed phase and amplitude profile. It is interesting that it is the only mechanism that produces profile modulation for nonrelativistic intensities, namely, for intensities less than  $10^{18} \text{ W/cm}^2$ . Since the field amplitude necessary to reach a certain level of ionization of the particular ions is known, the instant seed profile becomes strongly modulated and can be correlated with the corresponding ionization amplitude. Thus the seed modulation can be used to deduce the seed amplitude.

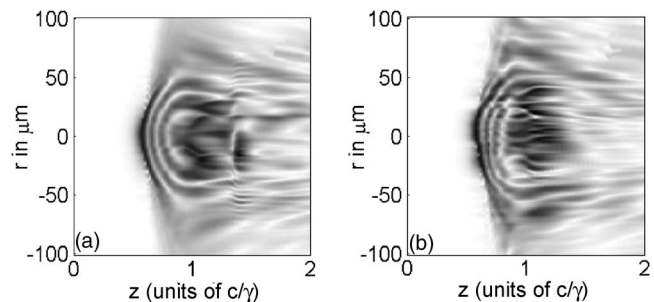


FIG. 6. Example of seed refraction in the case of the inhomogeneous plasma density with modulation 2.5% (left) and 5% (right). Seed and pump have transverse size  $60 \mu\text{m}$  FWHM.

## V. COMPARISON WITH EXPERIMENTAL RESULTS

The recent RBS amplification experiment [10,11] can be addressed in light of the effect considered here. The experiments were conducted in a plasma of propane gas jet with length about 2 mm. The plasma in the jet was created by relatively low power laser prepulse by impact ionization. The size of the plasma channel is of the order of  $80 \mu\text{m}$  in diameter and 1.3 mm effective length in the longitudinal direction. The plasma density was  $1.1 \times 10^{19} \text{ cm}^{-3}$ . The pumping pulse was focused somewhere inside the plasma (near seed entrance) and had maximum intensity  $10^{14} \text{ W/cm}^2$ . The seed pulse was driven from the opposite side and also was focused inside the plasma volume. The parameters of the seed were duration 550 fs, transverse size  $30 \mu\text{m}$  in focus, and intensity of the order of  $10^{12} \text{ W/cm}^2$ . Already the simple estimations show the possibility of achieving a nonlinear regime in the frame of these conditions.

The experiment exhibited saturation of the intensity of the amplified pulse. Also the transverse structure modification of the amplified seed was recorded. The dependence of output energy of the amplified seed versus its input energy is shown in Fig. 7. It can be seen that there is some sort of saturation for initial energies larger than 0.5 mJ. Such saturation can be explained by various processes: the reaching of a nonlinear level, the influence of plasma wave breaking, or the influence of additional ionization. However, none of these processes except ionization can lead to such abrupt saturation. It is

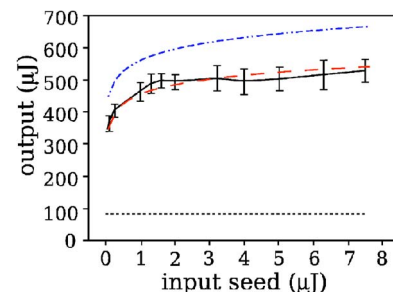


FIG. 7. (Color online) The dependence of the output energy of the amplified seed versus input energy (like Fig. 2 in [11]). The bend in dependence is clearly seen. Dash-dotted line is the result of a simulation without additional ionization. Dashed line is the result of a simulation with additional ionization. Dots at bottom denote level of noise.

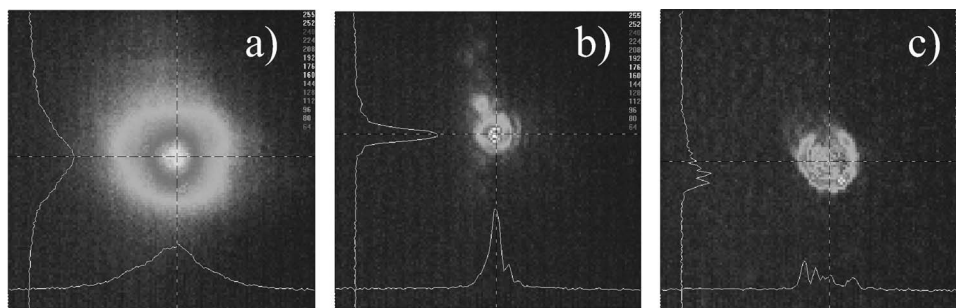


FIG. 8. The measurement of the transverse profile of the seed in the experiment (similar to Fig. 4 in [11]). Left picture (a) represent the case of the negligible amplification of the seed. Central picture (b) shows large RBS amplification of the seed. Right picture (c) shows the transverse profile of the seed (pump has qualitatively the same profile) before interaction in the plasma.

related to the fact that in the nonlinear regime ( $b_{max} > a_0$ ) and in the regime of wave breaking [ $b_{max} > (\omega_p / \omega_0)^2$ ] the amplitude and energy of the seed still grow. However, the difference from the linear regime is that growth is linear in distance or time rather than exponential. In the case when the additional ionization takes place, the limitation of the seed amplitude is governed by the ionization threshold. The growth of the energy in this case is possible only due to lengthening of the pulse. But the presence of plasma wave breaking prevents the lengthening of the pulse over several (about two) inverse increments.

One explanation of the saturation effect exhibited in Fig. 7 is that the output energy is limited by twofold ionization of the carbon ions by the seed pulse. The threshold of the second ionization of carbon is approximately equal to  $(3-5) \times 10^{14} \text{ W/cm}^2$  as follows from Eq. (10). This power density can be deduced easily by estimations:

$$W \approx \frac{0.5 \text{ mJ}}{(\pi/4)(20 \text{ } \mu\text{m})^2 0.4 \text{ ps}} \approx 4 \times 10^{14} \text{ W/cm}^2. \quad (13)$$

Note that both estimates show the achievement of the nonlinear regime of RBS amplification, i.e.,  $b_{max} > a_0$ .

There is another point—the large role played by ionization in limiting the output energy in this experiment. As we note in Sec. IV the transverse profile of the seed becomes very sensitive to inhomogeneity of the pump profile or plasma density if additional ionization occurs. The pump has a ragged transverse profile [see Fig. 8(c)], so we should expect transverse inhomogeneity of the seed in the presence of additional ionization. Alternatively, if no additional ionization is present the transverse profile of the seed should be smooth. Indeed, the seed profile is smooth in the case of low amplification [see Fig. 8(a)] when there is no additional ionization by the seed. This corresponds to averaging of the seed amplitude over many speckles (inhomogeneities) of the pump. On the other hand, the seed profile is jagged in the case of large amplification [see Fig. 8(b)] when additional ionization should occur (see Sec. IV). Thus, the raggedness of the output pulse corresponds to our understanding of the physical processes involved.

## VI. CONCLUSION

We have considered here the influence of additional ionization on the RBS amplification process in the case of par-

tially ionized gases. We found that plasma density growth due to ionization breaks down the Raman resonance. This leads to saturation of the Raman amplification if the beam intensity exceeds the ionization threshold. The critical intensity is calculated by summing up the amplitude of both the seed and pump waves. There are two main possibilities for avoiding this limitation: to use pure hydrogen plasmas or to use plasmas with a high-order preionization stage, so that the ionization threshold is much higher than the expected signal intensity. The last possibility was used in a recent capillary experiment [16] where a three times ionized argon plasma was used for intensities anticipated to be on the order of  $10^{14} \text{ W/cm}^2$ .

Using a mixture of gases will not compensate sufficiently the additional ionization. The cyclic process of ionization and frequency shift, followed by amplification of the frequency-shifted radiation and further ionization, does not lead to highly compressed and high-intensity output pulses. To maximize amplification the added ions should not exceed 3% of the bulk plasma ions.

The presence of any inhomogeneities of pump or plasma density in the transverse direction leads to modulative distortion of the seed phase and amplitude profile and produces further seed refraction. We suggest that this distortion might be useful for diagnostic purposes. We note that it is the only mechanism of the seed profile modulation that is possible in the absence of self-action through the relativistic nonlinearity. Therefore one can conclude that the ionization threshold has been exceeded if the transverse profile is strongly modulated. Hence one can estimate the output intensity since the value of intensity for each ionization threshold is well known.

To access the nonlinear regime of RBS amplification requires that the intensity of the output pulse be larger than the pumping pulse. Since the modulation of the ionizing plasma is the signature of the amplitude we can calculate that the output pulse then exceeds the pump pulse by a factor of 3. This would occur as the nonlinear regime is accessed.

The work was supported by RFBR Grant No. 05-02-17367a, the U.S. DOE under Contract No. DE-AC02-76-CHO3073, the U.S. DARPA, and in part by the National Nuclear Security Administration under the Stewardship Science Academic Alliances program through DOE Research Grant No. DE-FG52-04NA00139.

- [1] V. M. Malkin, G. Shvets, and N. J. Fisch, *Phys. Rev. Lett.* **82**, 4448 (1999).
- [2] V. M. Malkin, G. Shvets, and N. J. Fisch, *Phys. Rev. Lett.* **84**, 1208 (2000).
- [3] G. Shvets *et al.*, *Phys. Rev. Lett.* **81**, 4879 (1998).
- [4] V. M. Malkin and N. J. Fisch, *Phys. Plasmas* **8**, 4698 (2001).
- [5] G. M. Fraiman, N. A. Yampolsky, V. M. Malkin, and N. J. Fisch, *Phys. Plasmas* **9**, 3617 (2002).
- [6] Yu. A. Tsidulko, V. M. Malkin, and N. J. Fisch, *Phys. Rev. Lett.* **88**, 235004 (2002).
- [7] N. J. Fisch and V. M. Malkin, *Phys. Plasmas* **10**, 2056 (2003).
- [8] A. A. Balakin, G. M. Fraiman, N. J. Fisch, and V. M. Malkin, *Phys. Plasmas* **10**, 4856 (2003).
- [9] A. Solodov, V. M. Malkin, and N. J. Fisch, *Phys. Plasmas* **10**, 2540 (2003).
- [10] Y. Ping *et al.*, *Phys. Rev. Lett.* **92**, 175007 (2004).
- [11] W. Cheng *et al.*, *Phys. Rev. Lett.* **94**, 045003 (2005).
- [12] R. L. Berger, D. S. Clark, A. A. Solodov, E. S. Valeo, and N. J. Fisch, *Phys. Plasmas* **11**, 1931 (2004).
- [13] D. S. Clark and N. J. Fisch, *Phys. Plasmas* **9**, 2772 (2002).
- [14] D. S. Clark and N. J. Fisch, *Phys. Plasmas* **10**, 4837 (2003).
- [15] L. V. Keldysh, *Sov. Phys. JETP* **20**, 1307 (1965); M. V. Ammosov, N. B. Delone, and V. P. Krainov, *ibid.* **64**, 1191 (1986).
- [16] A. A. Balakin, D. V. Kartashov, A. M. Kiselev, S. A. Skobelev, A. N. Stepanov, and G. M. Fraiman, *Pis'ma Zh. Eksp. Teor. Fiz.* **80**, 15 (2004) [*JETP Lett.* **80**, 12 (2004)].